

OPEN

Myofascial trigger points alter the modular control during the execution of a reaching task: a pilot study

Tommaso Geri^{1,3*}, Leonardo Gizzi^{2,3}, Anna Di Marco¹ & Marco Testa¹

Myofascial trigger points (TP) constitute a conundrum in research and clinical practice as their etiopathogenesis is debated. Several studies investigating one or few muscles have shown that both active and latent TP causes an increased muscle activity, however the influence of TP on modular motor control during a reaching task is still unclear. Electromyographic signals, recorded from the muscles of the shoulder girdle and upper arm during a reaching task, were decomposed with Non-Negative Matrix Factorization algorithm. The extracted matrices of motor modules and activation signals were used to label the muscles condition as dominant or non-dominant. The presence of latent and active TP was detected in each muscle with manual examination. Despite a similar muscle activity was observed, we found that muscles with active TP had increased weighting coefficients when labeled in the dominant condition. No influences were found when muscles were in the non-dominant condition. These findings suggest that TP altered the motor control without co-contraction patterns. As a preliminary evidence, the present results suggest that the increased weighting coefficients in presence of TPs are associated with an alteration of the modular motor control without affecting the dimensionality of motor modules for each individual and reciprocal inhibition.

Trigger Points (TPs) are clinical entities commonly found in several musculoskeletal conditions as well as in healthy subjects¹. A TP is defined as a “hyperirritable spot in skeletal muscle that is associated with a hypersensitive palpable nodule in a taut band”². It can have two states according to the reproduction of the patient’s current or past symptoms (active TP) or not (latent TP) upon palpation³. Other features, such as a tender spot within a taut band, referred pain, and the presence of a local twitch response are common to the two states. Some explanations have been advanced to describe the development of TPs and their role on musculoskeletal pain^{4–11}, however there is debate on the origin of the primary nociceptive input causing the sensitization of the CNS (Central Nervous System) that leads to spot tenderness and referred pain^{12,13}.

The characteristic motor signs of a TP are the taut band and the local twitch response. The taut band is likely due to the Spontaneous Electrical Activity (SEA) observed at rest at the site of TP¹⁴, which is considered as extrafusal or intrafusal according to the withstanding hypotheses. The integrated trigger point hypothesis considers an extrafusal origin of the SEA as the combination of miniature endplate potentials and endplate spikes that cause an abnormal acetylcholine release due to muscle damage occurring in extraordinary activities or following a trauma¹⁵. On the other hand, it has also been suggested that SEA may be the electrical activity of muscle spindles which constitute the nociceptive locus from which TP and myofascial pain begins⁶. The local twitch response is commonly seen as an augmented arch reflex response, intended as stretch^{4,5} or withdrawal reflex⁷.

Motor alterations were found also for latent TPs^{16–18} and characterized both as “within-” and “between-muscles”. Within-muscle alterations comprise higher muscle spindle sensitivity, with higher amplitude and lower threshold of the H-reflex¹⁹, and increased metabolic fatigability¹⁸. Between-muscles alterations have been reported as either an increase in the activity of antagonist²⁰ as well as synergistic muscles¹⁷ or as a delayed activation with respect to the other agonist muscles²¹ of the muscle containing the TP. These phenomena are also

¹Department of Neuroscience, Rehabilitation, Ophthalmology, Genetics, Maternal and Child Health (DINOEMI), University of Genova, Campus of Savona, Genova, Italy. ²Institute for Modelling and Simulation of Biomechanical Systems, Continuum Biomechanics and Mechanobiology Research Group, University of Stuttgart, Stuttgart, Germany. ³These authors contributed equally: Tommaso Geri and Leonardo Gizzi. *email: tommaso.geri@gmail.com

Variable	N	Mean (SD)	Min	Max
Age (years)	15	28.13 (4.02)	22	34
Weight (Kg)	15	66.33 (11.18)	51	90
Height (cm)	15	171.2 (8.28)	160	186
VAS (0–10)	15	1.65 (1.88)	0	5.90
EQI (0–1)	15	0.89 (0.09)	0.76	1
NBQ – Functioning subscale (0–40)	15	3.33 (3.74)	0	10
NBQ – Anxiety subscale (0–20)	15	2.86 (3.38)	0	10
QuickDASH (11–55)	15	11.93 (1.16)	11	14
TSK (13–52)	15	16.47 (5.08)	13	31
PCS (0–52)	15	3.67 (3.87)	0	11

Table 1. Demographic variables and self-reported questionnaire scores. EQI, EuroQol Index, range from 0 (worst) to 1 (best); NBQ, Neck Bournemouth Questionnaire, subscales range from 0 (best) to 20/40 (worst); PCS, Pain Catastrophizing Scale, range from 0 (best) to 52 (worst); QuickDASH, Quick Disability of the Arm, Shoulder and Hand questionnaire, range from 11 (best) to 55 (worst); SD, Standard Deviation; TSK, Tampa Scale for Kinesiophobia, range from 13 (best) to 52 (worst); VAS, Visual Analogue Scale for pain intensity, range from 0 (best) to 10 (worst).

associated with a heterogeneous redistribution of activity of the other muscles during, for example, either slow²¹ or rapid²² arm elevation. This body of evidences may suggest that the nociceptive afferents from a TP induce alterations of the spinal circuitry whose efferent pathway causes a focal dystonia of the muscle involved¹⁰.

The CNS accomplishes the problem of controlling its numerous degrees of freedom during the continuous interaction with the environment by controlling a small set of elemental variables, also called motor modules²³. A motor module is a group of muscles controlled as a single unit²⁴ that is spatially and temporally characterized through the directional tuning of its weighting and timing coefficients, respectively²⁵. This approach has already been used to describe complex human motor behaviors like walking, in infants²⁶, healthy adults²⁷ and neurological patients²⁸; reaching task, in healthy^{29–31} and stroke subjects³²; and in presence of various musculoskeletal pain syndromes³³. Despite an influence of TP on motor modules has been hypothesized¹⁷, an investigation of the influence of TP at the level of modular motor control has not been performed so far.

In this study we aimed at exploring the role of active and latent TPs on the modular control of reaching movements. Upper limb muscular activities from the shoulder girdle and arm muscles were analyzed by means of Non-negative Matrix Factorization (NMF)³⁴ and dimensionality of control, while weighting and timing coefficients were extracted. The results were interpreted in light of the presence or absence of TPs. We hypothesized that the presence and number of TP may alter the individual dimensionality of the motor modules (Hypothesis 1). Furthermore, we expected that the presence of TPs altered the weighting coefficients of motor modules, possibly influencing the weighting coefficient of the hosting muscle in each synergy (Hypothesis 2). Moreover, we investigated whether muscle activity was also altered across muscles with or without TPs (Hypothesis 3). Finally, we generated a random presentation of TPs among the investigated muscles to understand whether our results might be influenced by a spurious association due to flaws in the palpation-based diagnosis of TPs (Hypothesis 4).

Results

Subjects. The 15 participants (7 F) had an average age of 28.13 ± 4.02 years. Six participants (3,7,9,10,12,14) reported musculoskeletal pain of the upper quarter, subject 8 a history of headaches and subject 13 of low back pain. The remaining 7 subjects had no history of musculoskeletal pain. The remaining demographic variables and scores of self-reported questionnaires are reported in Table 1.

Trigger points detection. The presence of TP is reported for subjects and muscles in Table 2. Subject 4 had no TPs detected in the muscles examined, two subjects had only one active TP each, while seven subjects had only latent TPs. The remaining 5 subjects had both active and latent trigger points (Table 2). The muscles with the highest number of both active and latent TPs were the SCOM (4 ACT, 5 LAT) and the TLO (2 ACT, 7 LAT). The muscles with active and latent TPs were, respectively, 13 (6%) and 50 (25%) on a total of 195 examined muscles.

Motor pattern and kinematics. A representative example of the time profiles of x -, y -, z -accelerations for all subjects and angles is reported for the wrist inertial sensor as it was considered the most able to detect inter-individual kinematic variability (Fig. 1).

Figure 1 In terms of influence of TP on the COV of x -, y -, z -accelerations, roll, pitch, and yaw, there were no effects due to the number of TPs for all sensors and movement directions (X^2 of all tests with $P > 0.05$). These results indicated that the experimental design allowed the subjects to perform the reaching tasks with similar kinematic and without different movement patterns despite the different distribution of TPs.

Dimensionality and similarity across-subjects. The structure of motor modules varied among subjects, which shown that a different dimensionality was needed when applying the inflexion point method individually. For instance, two to five modules were detected (S01 = 3, S02 = 2, S03 = 3, S04 = 3, S05 = 4, S06 = 2, S07 = 3, S08 = 5, S09 = 3, S10 = 2, S11 = 4, S12 = 5, S13 = 4, S14 = 4, S15 = 3). The regression analysis shown the absence

Subject	VAS	ACT (muscle)	LAT (muscle)
01	0	0	3 (BS, TM, SCOM)
02	0	0	4 (BR, TM, TLO, TU)
03	3.8	1 (DA)	1 (TLO)
04	0	0	0
05	0	0	2 (PM, TU)
06	0	0	2 (DP, PM)
07	5.9	1 (TM)	5 (BS, PM, SCOM, TLO, TU)
08	3	0	8 (BS, BR, DP, TM, PM, SCOM, TLO, TU)
09	3.7	0	8 (BS, BR, DM, DP, PM, SCOM, TLA, TLO)
10	1.5	1 (SCOM)	5 (DP, PM, TLA, TLO, TU)
11	0	1 (SCOM)	0
12	2	1 (SCOM)	0
13	2	4 (BR, PM, TLA, TLO)	4 (BL, BS, DA, SCOM)
14	2.8	4 (DM, TM, SCOM, TLO)	4 (BS, TL, PM, TU)
15	0	0	4 (BL, BS, TM, TLO)

Table 2. Result of muscle palpation for TP detection. ACT, Active trigger point; BL, Biceps Long head; BS, Biceps Short head; BR, Brachioradialis; DA, Deltoid Anterior; DM, Deltoid Middle; DP, Deltoid Posterior; LAT, Latent trigger point; TL, Trapezius Lower; TM, Trapezius Middle; PM, Pectoralis Major; SCOM, Sterno-Cleido-Occipito-Mastoideus; TLA, Triceps Lateral head; TLO, Triceps Long head; TP, Trigger Point; TU, Trapezius Upper, VAS, Visual Analogue Scale.

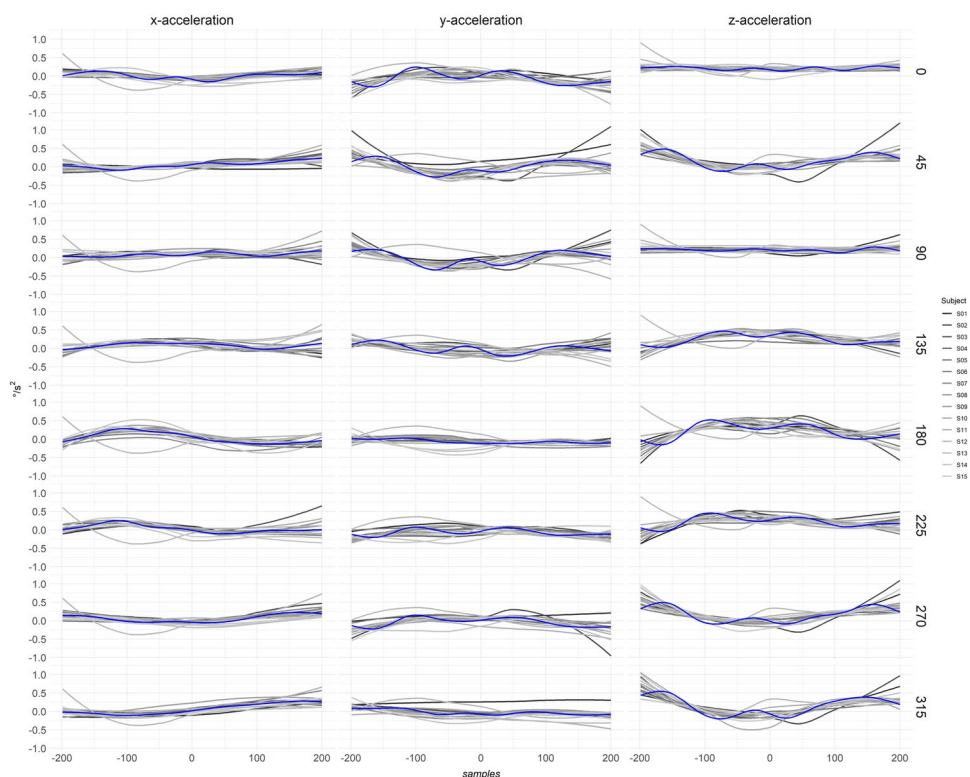


Figure 1. Time-profiles of x -, y -, z -accelerations of the wrist inertial sensor. In each column, the raw data of the kinematic variable is plotted versus the samples. The blue line represents the averaged value. The different number of samples from the one of the activation signals (see Fig. 3) is due to the different sampling frequency of the inertial sensor acquisition system. Each subject is represented by a line shaded in grey scale. Please note that the order of target is reported in degrees of a cartesian plane, therefore the order of target from top to bottom is 3, 2, 1, 8, 7, 6, 5, 4.

of any correlation between dimensions and number of TP (Pearson's $r = 0.10$, $P = 0.72$) or the presence of active TP (Pearson's $r = 0.30$, $P = 0.26$).

The curve of the VAF values averaged across subjects shown a change in slope at 3 factors (VAF = 0.77 ± 0.06 , see Supplementary Fig. S1). In order to test Hypothesis 2, the 3 motor modules extracted afterwards for all the

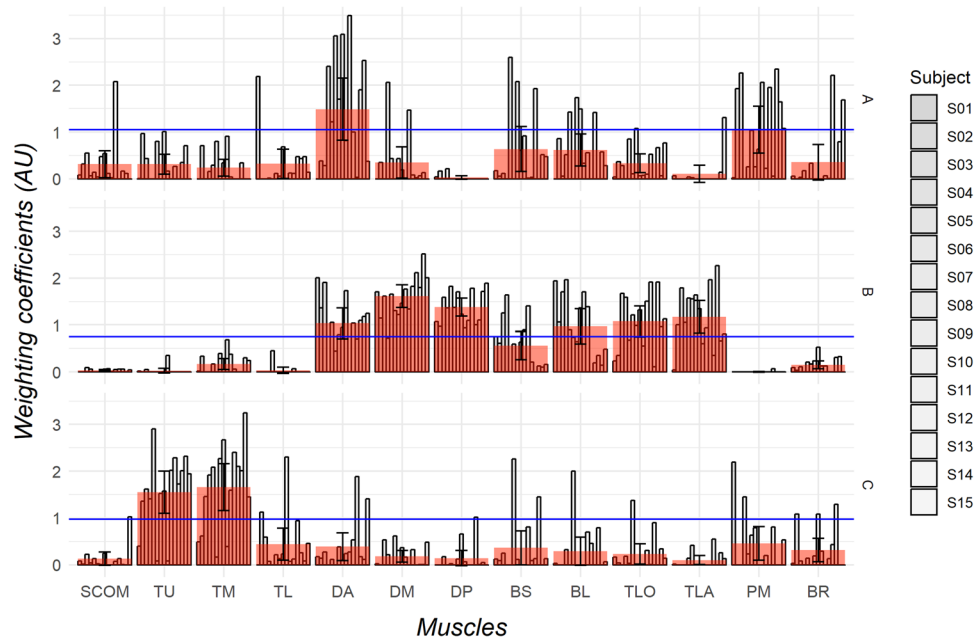


Figure 2. Motor modules retrieved from dimensionality analysis. Weighting coefficients are plotted for each subject and the mean with standard error in each synergy is superimposed for each muscle to show which are the dominant muscles for each synergy. Module A had the DA as dominant muscle, Module B had the DA, DM, DP, BL, TLO, and TLA muscle; and Module C had the TU and TM muscles. Note that despite the mean indicate an averaged dominant muscle, some subjects may have lower or higher weighting coefficients for that muscle (see Supplementary Fig. S2). Modules A, B, and C are described on the right. AU, Arbitrary Unit; BL, Biceps Long head; BS, Biceps Short head; BR, Brachioradialis; DA, Deltoid Anterior; DM, Deltoid Middle; DP, Deltoid Posterior; TL, Trapezius Lower; TM, Trapezius Middle; PM, Pectoralis Major; SCOM, Sterno-Cleido-Occipito-Mastoideus; TLA, Triceps Lateral head; TLO, Triceps Long head; TU, Trapezius Upper.

subjects were coupled according to their similarity. Despite the high inter-subjects variability, the average NDP (calculated using Subject-8 as reference) was 0.73 ± 0.14 .

Motor modules and directional tuning. The 3 motor modules are reported in Fig. 2 across subjects and with a superimposed global value calculated as mean and standard error across muscles. Motor modules were arbitrarily called A, B, C and dominant muscles for each subject were established with respect to the criterion of a weighting coefficient 30% higher than the maximum value within each module (solid horizontal blue line in Fig. 2). The weighting coefficients were similar among male and females.

Figures 2 and 3 displays the time profile of the activation signals of the 3 modules for each angle (directional tuning).

Statistics. The reduced model resulted in a significant interaction between TP presence and muscle condition on the weighting coefficients ($AIC = 352.5$, $X^2(3) = 916.39$, $P < 0.001$). The post-hoc analysis of the interactions revealed a significant difference when the muscles were in the dominant condition between ACT TP and LAT TP (Mean Difference (MD) = 0.6, 95%CI 0.32–0.78, $P < 0.001$) and between ACT TP and absence of TP (MD = 0.4, 95%CI 0.21–0.63, $P < 0.001$). The ES of this interaction was 0.46. No difference was observed in the dominant muscle between LAT TP and absence of TP (MD = -0.1, 95%CI = -0.26–0.01, $P = 0.05$, ES = -0.12). When the muscle with TP was in the non-dominant condition, no differences were found between ACT TP and LAT TP (MD = -0.1, 95%CI = -0.20–0.06, $P = 0.29$), ACT TP and absence of TP (MD = 0, 95%CI = -0.17–0.08, $P = 0.5$) and LAT TP and absence of TP (MD = 0, 95%CI = -0.04–0.09, $P = 0.44$) (Fig. 4). The marginal and conditional R-squared of the reduced model were 0.79 and 0.80, respectively, thus indicating that both the fixed and the random effects explained a significant proportion of variance of the fitted model. The diagnostics run on this model indicated no significant deviation from the normality assumptions (see Supplementary Figs S5–S10).

The analysis of RMS of each muscle displayed no difference in muscle activity patterns as no interaction between presence of TP, angles and modules was detected ($AIC = 2039.7$, $X^2_{(168)} = 115.65$, $P = 0.99$) (Fig. 5).

Two thousand grids simulating the presence of TP were randomly generated and only 7 (0.0035%) datasets gave a result within the 95% CI estimates derived from the original data. Therefore, the hypothesis that a significant result may arise from a spurious association between TPs detected with manual palpation and weighting coefficients of muscles within motor modules was rejected.

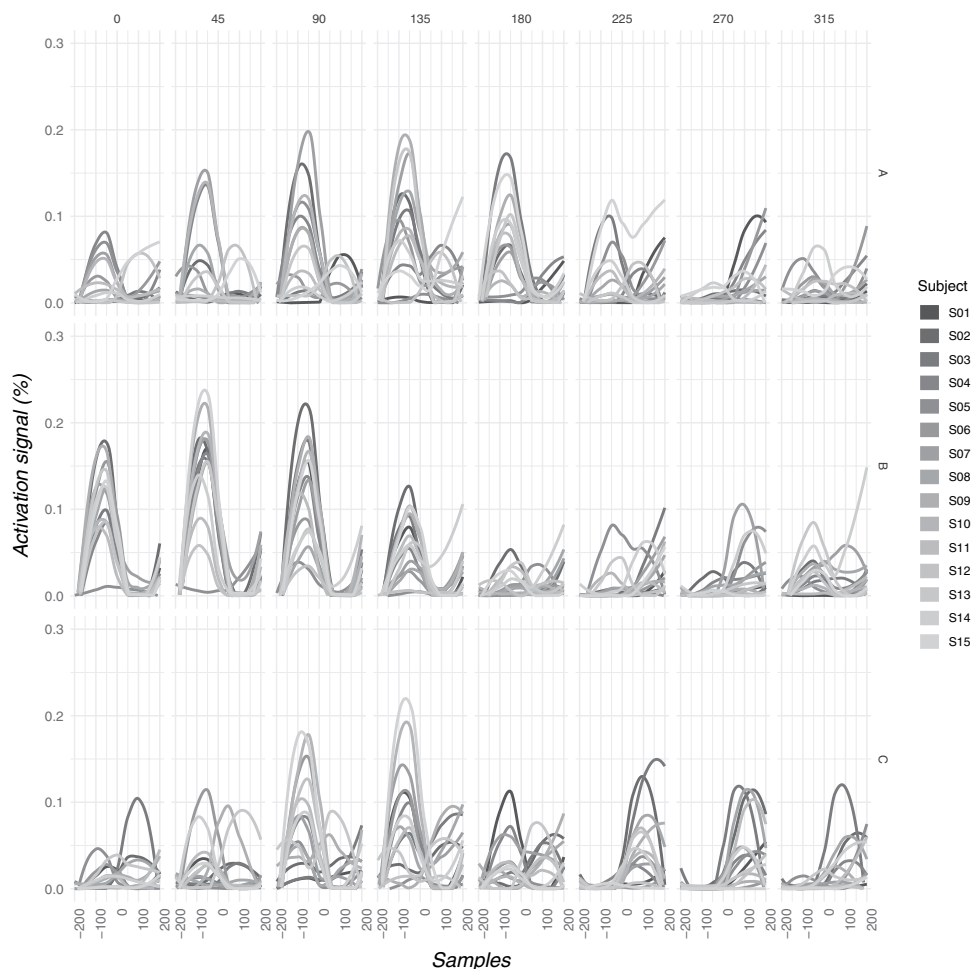


Figure 3. Time-profiles of the activation signals of all subjects for all motor modules and angles. Note that modules 2 and 3 overlaps for certain angles: this happened because some subjects achieved the criterion at 2 modules but 3 modules were extracted for all subjects in order to have comparable and meaningful data. Modules A, B, and C are described on the right. Please note that the order of target is reported in degrees of a cartesian plane, therefore the order of target from left to right is 3, 2, 1, 8, 7, 6, 5, 4.

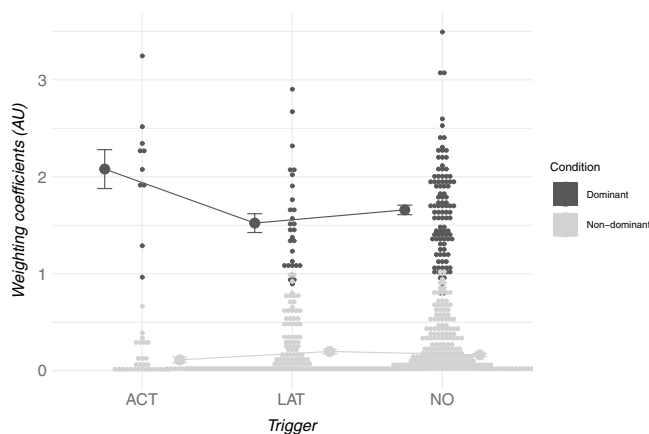


Figure 4. Second order interaction plot representing the influence of active trigger points on muscles in the dominant condition (black) while in the non-dominant condition (grey) there is no difference between muscles with or without trigger points. Small dots aligned above the three columns of trigger point presence conditions (ACT, LAT, NO) represent every single observation. Big black dots on the left and the big grey dots on the right of each column represented the mean values with error bars predicted by the mixed model. ACT, Active trigger point; AU, Arbitrary Unit; LAT, Latent trigger point; NO, Absence of trigger point.

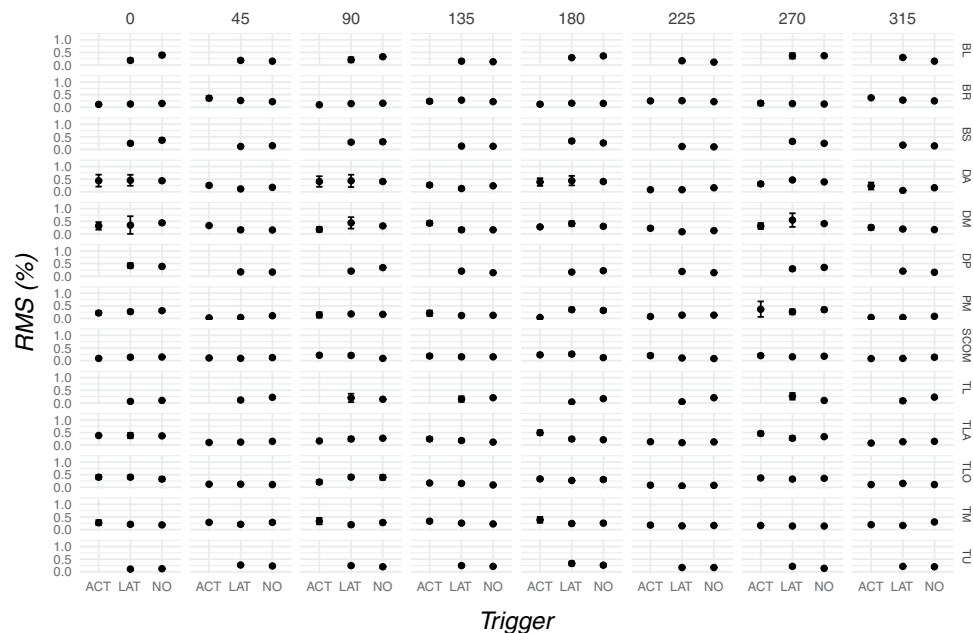


Figure 5. Mean and error bars of RMS of the three TP conditions (bottom) of each muscle (right) represented for every target (top). Increased muscle activities in presence of active TP were revealed for the TLA muscle at 180° and the DM muscle at 135°. A significant RMS decrease associated with active TP was detected for the PM muscle at 180°. Please note that the order of target is reported in degrees of a cartesian plane, therefore the order of target from left to right is 3, 2, 1, 8, 7, 6, 5, 4. ACT, Active trigger point; BL, Biceps Long head; BS, Biceps Short head; BR, Brachioradialis; DA, Deltoid Anterior; DM, Deltoid Middle; DP, Deltoid Posterior; LAT, Latent trigger point; TL, Trapezius Lower; TM, Trapezius Middle; PM, Pectoralis Major; RMS, Root Mean Square; SCOM, Sterno-Cleido-Occipito-Mastoideus; TLA, Triceps Lateral head; TLO, Triceps Long head; TU, Trapezius Upper.

Discussion

The present investigation on the influence of TPs on the modular control of reaching movements found a preliminary evidence that the weighting coefficients of dominant muscles hosting an active TP were higher than those of the dominant muscles hosting a latent TP or without TP, while no differences were detected among muscles in non-dominant condition. Furthermore, the regression analysis between dimensionality of modules structure and TP presence showed no correlations nor the analysis of RMS showed any influence of TP presence across muscles and angles. Previous literature already demonstrated an influence of TP at multi-muscular level on the muscle recruitment order during dynamic tasks^{21,22}, even though it was still unclear whether a TP altered the EMG activity of the agonist muscle^{16,17} and whether these alterations influenced the modular organization of movement in terms of weighting coefficient of the involved muscle. This preliminary evidence expands the understanding of the topic of TPs for their etiopathogenesis and for their clinical and research management.

The analysis of the structure of motor modules revealed that the presence of TPs left the control of the modular architecture of shoulder girdle and upper limb muscles unaltered, as the 3 modules structure was similar to a previous study on anti-gravitational reaching task using the inflexion point method²⁵. The number of extracted modules varied among subjects, suggesting that TP presence may alter the dimensionality of the individual modules structure. A recent review reported an inconsistent evidence of the influence of musculoskeletal pain on the number of modules extracted according to VAF values, with studies reporting a decreased, an increased or a similar number of modules³³. The regression analysis reported herein showed no correlations between individual number of extracted modules and number of TP or presence of active TP. Despite heterogeneous dimensionality was present, it was probably unaffected by TP; however, further studies are needed to clarify this issue. Furthermore, none of the subjects showed an altered control of motor modules in contrast to what is seen with motor cortical damage³².

Despite the evidence of an alteration of weighting coefficients is inconsistent when muscle pain is induced experimentally³³, the present results highlight for the first time that TPs influence how much a muscle is involved in a module. The model run on the influence of TP presence (ACT, LAT, NO) on the weighting coefficients, used to understand the amount of muscle involvement within a module confirmed our Hypothesis 2 that a TP altered the weighting coefficients of the muscle with the TP when it is involved in the motor modules as dominant. However, the absence of a difference in the non-dominant condition indicates that when a muscle participated in a motor module without a dominant role, the presence of TP left its weighting coefficient unaltered. This preliminary evidence shows that TP did not induce a pattern of co-contraction across muscles and, consequently, contradicts a previous study that attributed the increased activity of the antagonist muscle with TPs to a dysregulation of the reciprocal inhibition²⁰.

Our results on RMS agree with previous studies that found no increased muscle activity in presence of latent TP^{16,17}. Whilst other Authors reported an increased muscular activity of muscles hosting a latent TP^{17,18,20} their results are likely attributable to a higher selectivity of intramuscular EMG, compared to the bipolar superficial EMG in our study. As increased twitch force has been reported despite no changes in superficial EMG³⁵, mechanomyography may be useful to study muscles with latent TP.

The higher activity of the agonist muscles with active TPs has been ascribed to a central alteration of muscle tone³⁶ that leads to a higher recruitment of the associated alpha-motoneurons either at rest, as demonstrated by the presence of the SEA¹⁵, and during reaching tasks. Some authors have hypothesized an involvement of the Ia-inhibitory interneuron²⁰, the Renshaw cells¹⁹ and the gamma-motoneurons⁶, while others have suggested a direct dysfunction occurring at the motoneuron soma⁷. Furthermore, other authors have pointed out that the motoneuron is also aided by an altered nociceptive pathway arising from lesions of the neural tissue³⁷ or of the tissues segmentally related to the innervation level of the muscle with TP⁸ or from the direct compression of the nerve roots at the vertebral level, which the muscle with TPs segmentally belongs to⁹. Despite the fact that all the proposed spinal neurophysiological mechanisms point to an altered muscle tone causing an unpredictable muscle activation in presence of TPs, this preliminary study shows that the alteration is evident also at the level of motor modules, as it emerged only in the module when the muscle was dominant, becoming consequently an activity-driven alteration.

All the hypotheses on TP formation assume that a TP is born in its latent state after prolonged or unaccustomed exercise, low-load repetitive exercise, trauma or sustained stress that leads to muscle damage (or other nociceptive sources).

After a TP has formed, it acts as a peripheral nociceptive source and may start the abovementioned alterations of the spinal circuitry that, when fatigue arises, result in an overall increased EMG activity and decreased firing rate of the involved motor units³⁸. This motor behaviour resembles what is observed during the motor adaptation to pain when the loss of force output due to a generalized reduction of discharge rate³⁹ in the painful muscle is compensated via a heterogeneous recruitment of additional motor units⁴⁰ in the acute phase, and a reduced complexity of motor unit recruitment⁴¹ in the chronic phase. These mechanisms explain the increased activity of agonist muscles with active TPs, as the criterion discriminating active from latent TPs is the reproduction of familiar pain. In contrast, the increased EMG activity occurring in the muscle with latent TP has been linked to the recruitment of additional motor units that allows the achievement of a similar force output¹⁷. This concept is supported by several studies documenting a similar force in subjects with and without latent TPs during isometric or dynamic contractions tasks^{16,17,21}. The present study enriches the perspective on TPs as they increased also the weighting coefficient of the dominant muscle of a module. Therefore, the contraction of muscle fibres typical of TPs may couple with the redistribution of muscles weighting coefficient within a module that recruits more the muscle with active TP. In this new perspective, TPs may represent the epiphenomenon of a motor re-organization occurring at the level of motor modules. Despite the understanding of the mechanism originating the dysfunctional motor module is beyond the observational purpose of this experiment, we can speculate that a common dysfunctional motor module may present across patients with different clinical scenarios and the associated TPs. For instance, the presence of specific TPs in individuals will emerge as the result of a complex interaction among the dysfunctional motor module, the individual characteristics (physical and cognitive) and the environmental context where the movement is executed. Accordingly, the heterogeneity of the alteration of motor modules in presence of muscular pain³³ may occur because researchers have focused their attention on finding similar motor alteration in patients with similar pain syndromes. However, it may be the case that a common dysfunction of motor modules may have heterogeneous clinical manifestations. This hypothesis may be tested by demonstrating that a sample of subjects with various nonspecific musculoskeletal disorders of the upper quadrant, such as neck, shoulder and arm pain, share common dysfunctional motor modules during the reaching task performed in this experiment. Therefore, future research in the field should consider the exploitation of dysfunctional motor modules as a new field of inquiry in presence of TP and musculoskeletal pain.

In clinical practice, the clinician usually selects the muscle supposed to be involved in the matching between the patient's pain quality and history, such as aggravating movements or postures, with the body map of referred pain pattern⁴². Once the muscle has been selected, then the clinician follows the muscle palpation to detect the typical clinical signs of the TP (e.g. local tenderness, taut band, patient's pain recognition and referral, local twitch response)³. If the muscle palpation gives positive findings, then the muscle is diagnosed as having an active TP. The treatment is often based on an iterative treat-and-reassess process wherein the clinician re-directs the treatment to other muscles, using the abovementioned reasoning, until the patient's symptoms are modified/disappeared. The treatment is often supported with stretching and strengthening of the muscle involved². This study provides preliminary evidence that the analysis of motor modules may reveal which is the dysfunctional muscle and whether the treatment has been effective in the restoration of an unaltered motor control. Furthermore, the understanding of the involved motor module may inform the selection of exercises that recruit specifically the affected motor module.

The potential limits of the study are related to the detection of TP with only one examiner and to the small sample size. The bias in palpating and detecting TPs was handled refitting the same model using a random generation of the observed TP frequencies. Even though it was not possible to analyze all the possible combinations, only a small and statistically significant proportion of the 2,000 generated datasets produced similar results as ours, supporting that the presence of any spurious association was unlikely. A small sample size may produce an underpowered study for the reported effects. However, the mixed model approach had satisfactory marginal and conditional R-squared (e.g. the degree to which the variables set as fixed or random effects explain the variance of the model). Furthermore, the ES for the difference between active TP versus latent or no TP was moderate. Another limitation of the study was related to the motor module decomposition that was obtained merging only two repetitions for each movement even though a higher number of repetitions is suggested to improve

decomposition quality⁴³. Therefore, further studies with bigger samples, established using the R-squared and ES reported in this article, and more repetitions are needed to test the Hypothesis 2 of this study that, at this time, suffered from an over-inflation of the results. Finally, only superficial muscles were studied as their palpatory examination of TP is comparable to the diagnosis made by ultrasound⁴⁴. It is possible that using intramuscular EMG and ultrasound identification of TP also in deep muscles may have revealed further findings, as superficial EMG may be biased by cross-talk effects of the muscle underneath the ones studied. However, at this time we preferred to not overcomplicate an initially explorative study.

In conclusion, the present study reported an increased weighting coefficient of muscle hosting active TPs when the muscle was dominant according to the modular control of movement. Further, TPs did not alter the dimensionality of modules structure nor muscle activity. The results expand the perspective on TP at a multi-muscular level suggesting the absence of a co-contraction pattern. The analysis of motor modules may assist clinicians in measuring the effectiveness of therapeutic interventions directed to TP.

Methods

Study design and setting. A cross-sectional study was performed at the research laboratory of the Campus of Savona, Department of Neurosciences, Rehabilitation, Ophthalmology, Genetic, Maternal and Child Health (DINOEMI) of the University of Genova. The study received approval by the Regional Ethical Committee (Liguria - P.R. 095REG2015). All participants signed an informed consent and were allowed to withdraw from the study at any time. The experiment was performed in accordance with relevant guidelines and regulations.

Study population. Fifteen volunteers aged 18–50 years, were recruited to form a convenience sample. As the focus of the experiment was to detect the influence that TPs have on motor control, people with or without musculoskeletal disorders were considered. Subjects were excluded if they showed relevant comorbidities (tumors, central or peripheral neurological disease, rheumatic diseases, previous surgery to the spine or upper limb, cardiovascular diseases) or were currently taking muscle relaxants, or other medications possibly influencing muscular activity or pain.

Baseline variables. Subjects filled up a self-report questionnaire to collect the following demographic variables: gender, age, weight, height, pain intensity and location on a body map.

To measure health-related quality of life in each subject, the following cross-culturally adapted and validated Italian questionnaires were administered: the EuroQoL Index (EQI) for the general health status⁴⁵, the Visual Analogue Scale for pain intensity⁴⁶, the Neck Bournemouth Questionnaire for neck pain functioning and anxiety⁴⁷, the QuickDASH for function of neck and upper limb⁴⁸, the Tampa Scale for Kinesiophobia to assess avoidance beliefs related to movement⁴⁹ and the Pain Catastrophizing Scale to assess biased beliefs regarding pain experience⁵⁰.

Trigger point detection. An experienced examiner (TG) detected the presence of active and latent TPs using the criteria proposed by the most recent consensus on TP diagnosis³. The TP palpation procedure was based on the Anatomical Landmark Framework (ALF) lines used to avoid electrode positioning over the innervation zone (see *Electrode positioning and EMG recordings paragraph*). During the palpation of each muscle, the following criteria were tested for:

1. spot tenderness present in a taut band,
2. familiar (active TP) or unfamiliar pain (latent TP) elicited by palpation of the tender spot
3. referred pain elicited by palpation of the tender spot,
4. local twitch response (visible or felt under the fingertip) elicited during snapping palpation.

A muscle was considered to host an active TP when all the criteria were met. The TP was labelled as latent when the first and fourth criteria were respected, and the second criterion was scored for unfamiliar pain³. For a latent TP, the presence of the third criterion was considered not relevant.

Despite the fact that aforementioned criteria provides an acceptable inter- and intra-rater reliability in the identification of TPs in the upper quadrant⁵¹, a statistic was performed to avoid any biased identification of TPs due to the presence of only one examiner (see *Statistical analyses paragraph*).

Experimental task. Subjects performed an upper limb reaching task in two ways: circular and random. A wood panel supported 9 targets that the subjects were requested to reach in a timely manner (Fig. 6a–c). Eight targets were arranged in a circumference at 45° intervals, whilst the ninth target constituted the centre of the circumference (Fig. 6a, see also Gizzi *et al.*⁵²). The height of the subject's seat was regulated to align the shoulder joint with the central target. The criterion established to adjust the radius was that subjects had to reach each target with a straight elbow whilst the hand moved approximately 45° away from the initial position. (Fig. 6b). For each target, the acquisition started with the subject sitting straight on a chair with their knees 90° flexed. An initial training session was administered to let the subject familiarize with the experimental setting and the task rhythm that was organized in four periods (Fig. 6c). For the circular task, the subjects reached all the targets in a clockwise direction consecutively starting from target 1. For the random task, the order of presentation of targets was randomized for all participants. In both tasks, subjects performed one repetition for each target. A rest period was provided after each set of movements to prevent fatigue. In the meantime, data was saved on a computer hard-drive for offline analysis. Only the EMG produced during transitions (i.e. second and fourth periods, Fig. 6c) was used for motor module decomposition.

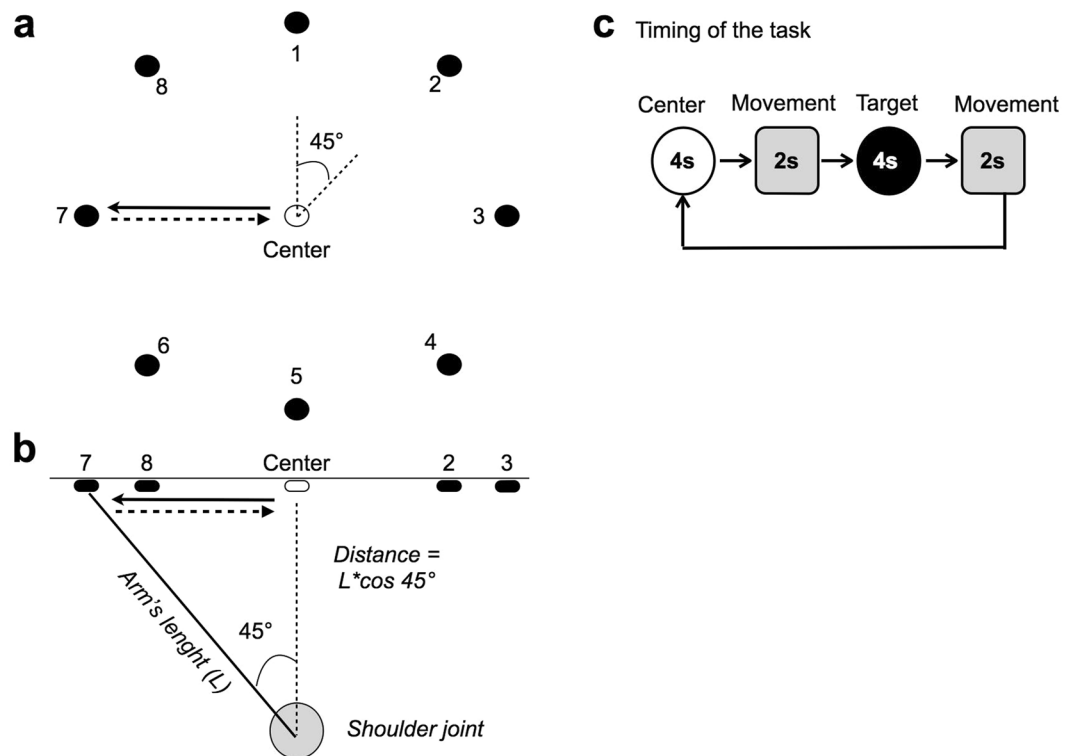


Figure 6. Experimental setup. (a) The wood panel had customized rails to adjust the radius of the circumference according to the distance between the shoulder joint and the central target to account for the inter-individual variability of arm's length. (b) Geometric description of the criterion used to set the distance between the shoulder joint and the central target. The subjects had to reach each target with a straight elbow whilst the hand moved approximately 45° away from the initial position. (c) The task rhythm was paced in four timeframes. In the first, the subject pushed the central button for 4 seconds while keeping the arm on the horizontal plane. In the second, the subject reached one radial target in about 2 seconds. In the third, the subject pressed the radial button for 4 seconds. In the fourth, the subject moved back to press the central target for about 2 seconds and then relaxed the arm.

Electrode positioning and EMG recordings. Pairs of Ag/AgCl electrodes (15×15 mm bipolar electrodes, Spes Medica, Genova, Italy) were positioned on the following 13 muscles of the right side (all the subjects were right-handed): upper, middle and lower trapezius (TU, TM and TL, respectively), anterior, middle and posterior deltoid (DA, DM, and DP), pectoralis major (PM), medial and lateral head of the biceps brachii (BS, BL), lateral and long head of the triceps brachii (TLA, TLO), brachioradialis (BR), and the sternal head of the sterno-cleido-occipito-mastoideus (SCOM). Skin was prepared by gentle abrasion with abrasive paste (Every, SpesMedica, Genova, Italy) and cleaned with water. Electrodes were positioned along the ALF following established criteria⁵³ to avoid positioning over the innervation zone. The ALF was marked with a blue pencil for all the muscles on each participant's skin at the beginning of the experiment and served also for TP detection. The signal quality achieved using these criteria varies from good to excellent for all muscles⁵⁴. The surface EMG acquisition (EMG-USB, OTBioelettronica, Turin, Italy) was synchronized with kinematic recordings. The EMG segmentation and computation of motor modules were performed in MATLAB (Matlab 2016b, the Mathworks, Natick, Massachusetts) via a custom made script.

Kinematic data recording. Subjects were equipped with inertial sensors (Xsens Technologies B.V, Enschede, The Netherlands) to record the motion of the arm using x -, y -, and z -acceleration profiles and 3D articular angles (roll, pitch, yaw). Inertial sensors were positioned on the posterior aspect of the distal third of the forearm and of the arm respectively, the top of the acromion, and the Lewis sternal angle.

The 3D characterization of movement allowed to select the portion of movement from which extracting the EMG signal (Fig. 6c). The Coefficient of Variation (COV) was estimated for each kinematic variable and used to assess whether the presence of TP altered the kinematic of the movement across subjects (*see Statistical analysis section*).

Preprocessing, segmentation and normalization of EMG signal. EMG data was band-pass filtered (10–450 Hz, 2nd order Butterworth filter) and then high-pass filtered (50 Hz, 2nd order Butterworth filter) to attenuate movement artifacts⁵⁵.

EMG segmentation was based on the start and the end of the movement, detected when the speed value exceeded the reference value of the standard deviation of the rest phase by over 5%. The influence of gravity on

the EMG was corrected according to d'Avella *et al.*⁵⁵. Briefly: the average rectified EMG value for each muscle was computed in two 300 ms windows (one prior to, and one after the completion of the movement). The two baseline values were linearly interpolated across the length of the movement, and the line was subtracted from the signal envelope (see below) on a sample-by-sample basis. The EMG data of each movement was first concatenated, and then full-wave rectified and low-pass filtered (5 Hz, 4th order Butterworth filter); the tonic activity for each movement was subtracted and individual movements were resampled to 200 samples⁵². Since NMF only works with non-negative data, the EMG values falling below zero after tonic activity subtraction were padded to zero⁵⁵. For each movement, the EMG was normalized using the average of the global maximum of the two trials after gravity compensation. The data from two trials for the same target were averaged. The amplitude of the muscular activity was estimated with the Root Mean Square (RMS) of the normalized EMG signal for each muscle. The RMS indicated the degree of muscular activation and is termed “muscle activity” throughout the manuscript.

Muscle synergies analysis and non-negative matrix factorization. The extraction of muscle synergies with Non-negative Matrix Factorization (NMF) followed well-established procedures^{28,52}. The NMF algorithm³⁴ was used to extract the motor modules from the segmented EMG signal. Each motor module is composed by a set of weightings (S , indicating the extent of mutual activation of different muscles within one synergy and termed “weighting coefficients” throughout the manuscript) and one of activation signals (P , which quantify the extent of recruitment of a given set of weightings over time) according to (1):

$$X(k) \approx X_r(k) = S \cdot P(k) \quad (1)$$

Since, while using NMF, the dimensionality of the solutions space is not known a priori, a number of synergy variable between 1 and 12 was computed and the dimensionality was chosen according to the following criterion: for each NMF run, the reconstruction quality of the original EMG by means of the extracted muscle synergies was assessed as the Variance Accounted For (VAF), defined as:

$$[\text{VAF} = 1 - \text{SSE}/\text{SST}]$$

where SSE is the Sum of Squared Error (computed as the difference between the reconstructed EMG signal and the original EMG data) and indicates the unexplained variance. SST is the Total Sum of Squares (calculated as the difference between each observation of the EMG data and its mean) and indicates the variance explained. The number of synergies to extract was determined using the inflexion point (e.g. change in slope) of the VAF curve averaged across subjects²⁵. The dimensionality was also determined for each subject separately and correlated using a regression analysis with the number of detected TP and with the presence or absence of active TPs.

The NMF was initialized with a seeding method of random generation of non-negative matrices and was run 10 times. The run with the best reconstruction quality (*see below*) was selected for further analyses.

The similarity of muscle weightings across subjects was assessed with the average Normalized Dot Product (NDP), calculated as the scalar product of two vectors of motor modules divided by the product of their norms^{30,52}. Each subject was iteratively isolated and used as a reference to compute the average NDP for all the others. The highest value was retained.

Statistical analyses. The free statistical software R version 3.4.1⁵⁶ was used for the statistical analyses. Demographic variables and questionnaire scores were reported as mean, standard deviation (SD), minimum and maximum values. The presence of active or latent TPs or their absence was reported as absolute frequency indicating the muscle involved for each subject.

The motor modules were summarized according to the data in matrix S (weights of motor modules) and matrix P (activation signals) to depict the structure of the synergies and their preferential activation in space. For the matrix S , a muscle was considered dominant for each subject in each module when its weight exceeded a threshold value calculated in percentage of the maximum weighting coefficient within each module⁵⁷, which in this study was set at 0.3. This kind of muscles labelling was needed to couple the presence of TP with the role that a muscle has within a module, as a TP may influence the weighting coefficients of a muscles either dominant or not in a module. For matrix P , the time-profile of module activation was displayed individually for each angle and module. The number of modules for each subject was correlated with the number of total TP and the presence of active TP using a linear regression analysis (Hypothesis 1).

The potential bias of the repeated measurements due to the study design and data extraction method was handled using a linear mixed model statistic performed with the package lme4 version 1.1-13⁵⁸ which allowed to take into account the variance due to the presence of multiple within subject factors (subject ID, muscles, motor modules, targets, sensor position). The model fit was tested with the Likelihood Ratio (LR) test of significance using the Maximum Likelihood (ML) estimator. The model with a significant Chi-squared (X^2) test and the lowest Akaike's Information Criterion (AIC) was retained for the analysis of the fixed effects. Significant higher order interactions were analysed with the least square means method with Kenward-Roger approximation of degrees of freedom using the package lmerTest version 2.0-33⁵⁹. The marginal and conditional R-squared were used as a measure of the proportion of variance of the model explained by, respectively, the fixed and random effects. Calculation was performed using Kagakawa and Schielzeth's method for mixed models implemented in the MuMIn package version 1.40.0⁶⁰. The Effect Size (ES) was calculated using the simr package version 1.0.5⁶¹. The P value was set to 5%. For the model diagnostics the normality assumptions were tested inspecting quantile-quantile plots of the residuals and of each level of the random effects structure⁶². The model linearity was deemed acceptable when the difference between the fitted values and the residual values was close to zero. The independence among fixed effects was tested using the Variance Inflation Factor (VIF); a VIF lower than 2 was needed to avoid collinearity, and if the VIF was higher than 2 the related fixed effect was dropped from the model

and the analysis of collinearity was re-run. Homoskedasticity assumption was confirmed when Levene's test⁶² on the model residuals was not significant.

An alteration of the subject's kinematic that may bias the conclusions drawn about the EMG decomposition was analysed after dichotomization of the subjects into two groups, classified as having active TP or not, respectively. A mixed model approach was used on the dependent kinematic variables (COV of x -, y - and z -accelerations, and roll, pitch and yaw) derived from the inertial sensors of each subject. For each kinematic variable, the group presence of TP (2 levels: ACT, NO) was treated as fixed effects while ID (15 levels), targets (8 levels: 0, 45, 90, 135, 180, 215, 270, 315), and sensor position (4 levels: sternum, shoulder, arm, and forearm) were treated as random effects. A non-significant X^2 test indicated the lack of kinematic alterations.

For the statistic of matrix S, Hypothesis 2 was tested using a mixed model approach on the weighting coefficients, with presence of TP (3 levels: ACT, LAT, NO), muscles condition (2 levels: DOMINANT, NON-DOMINANT) and modules (3 levels: A, B, C) as fixed effects and ID (15 levels) and muscles (13 levels) as random effects. Subject ID was not considered a random effect as its variance was 0. There was a significant interaction between TP, muscles condition and motor modules ($AIC = 301.26$, $X^2_{(9)} = 980.58$, $P < 0.001$, see Supplementary Fig. S3). However, the diagnostics revealed VIF values higher than 2 for either the single effects and for their interactions, therefore the model was re-run without the predictor module. Hypothesis 3 was tested with a mixed model approach on RMS values, with presence of TP (3 levels: ACT, LAT, NO), muscles (13 levels) and targets (8 levels) as fixed effects and ID (15 levels) as random effects.

In order to overcome the possible bias of the identification of TPs arising from the manual palpation executed by only one assessor, the analysis on matrix S was repeated with a random generation of 2,000 datasets of the TP presence to test Hypothesis 4. An acceptable result was considered when less than 5% of the random generated datasets gave results similar to those observed in the original data.

Data availability

The authors declare that data and materials are available to readers upon reasonable request.

Received: 30 January 2019; Accepted: 16 October 2019;

Published online: 05 November 2019

References

1. Lluch, E. *et al.* Prevalence, incidence, localization, and pathophysiology of myofascial trigger points in patients with spinal pain: A systematic literature review. *J Manipulative Physiol Ther.* **38**, 587–600 (2015).
2. Simons, D. G., Travell, J. G. & Simons, L. S. *Myofascial pain and dysfunction. The trigger point manual*. 2nd edn Vol.1 *Upper half of the body*. (Williams & Wilkins, 1999).
3. Fernandez-de-Las-Penas, C. & Dommerholt, J. International consensus on diagnostic criteria and clinical considerations of myofascial trigger points: A delphi study. *Pain Med.* **19**, 142–150 (2018).
4. Gerwin, R. D., Dommerholt, J. & Shah, J. P. An expansion of simons' integrated hypothesis of trigger point formation. *Curr Pain Headache Rep.* **8**, 468–475 (2004).
5. Partanen, J. End plate spikes in the human electromyogram. Revision of the fusimotor theory. *J Physiol Paris.* **93**, 155–166 (1999).
6. Partanen, J., Ojala, T. A. & Arokoski, J. P. Myofascial syndrome and pain: A neurophysiological approach. *Pathophysiology.* **17**, 19–28 (2010).
7. Hocking, M. J. Exploring the central modulation hypothesis: Do ancient memory mechanisms underlie the pathophysiology of trigger points? *Curr Pain Headache Rep.* **17**, 347 (2013).
8. Srbely, J. Z. New trends in the treatment and management of myofascial pain syndrome. *Curr Pain Headache Rep.* **14**, 346–352 (2010).
9. Gunn, C. Radiculopathic pain: Diagnosis and treatment of segmental irritation or sensitization. *Journal of Musculoskeletal Pain.* **5**, 119–134 (1997).
10. Rivner, M. H. The neurophysiology of myofascial pain syndrome. *Curr Pain Headache Rep.* **5**, 432–440 (2001).
11. Eloqayli, H. Subcutaneous accessory pain system (saps): A novel pain pathway for myofascial trigger points. *Med Hypotheses.* **111**, 55–57 (2018).
12. Quintner, J. L., Bove, G. M. & Cohen, M. L. A critical evaluation of the trigger point phenomenon. *Rheumatology (Oxford).* **54**, 392–399 (2015).
13. Dommerholt, J. & Gerwin, R. D. A critical evaluation of quintner *et al.*: Missing the point. *Journal of bodywork and movement therapies.* **19**, 193–204 (2015).
14. Hubbard, D. R. & Berkoff, G. M. Myofascial trigger points show spontaneous needle emg activity. *Spine (Phila Pa 1976).* **18**, 1803–1807 (1993).
15. Ge, H. Y., Fernandez-de-Las-Penas, C. & Yue, S. W. Myofascial trigger points: Spontaneous electrical activity and its consequences for pain induction and propagation. *Chin Med.* **6**, 13 (2011).
16. Barbero, M., Falla, D., Mafodda, L., Cescon, C. & Gatti, R. The location of peak upper trapezius muscle activity during submaximal contractions is not associated with the location of myofascial trigger points: New insights revealed by high-density surface emg. *Clin J Pain.* **32**, 1044–1052 (2016).
17. Ge, H. Y., Monterde, S., Graven-Nielsen, T. & Arendt-Nielsen, L. Latent myofascial trigger points are associated with an increased intramuscular electromyographic activity during synergistic muscle activation. *J Pain.* **15**, 181–187 (2014).
18. Ge, H. Y., Arendt-Nielsen, L. & Madeleine, P. Accelerated muscle fatigability of latent myofascial trigger points in humans. *Pain Med.* **13**, 957–964 (2012).
19. Ge, H. Y., Serrao, M., Andersen, O. K., Graven-Nielsen, T. & Arendt-Nielsen, L. Increased h-reflex response induced by intramuscular electrical stimulation of latent myofascial trigger points. *Acupuncture in medicine: journal of the British Medical Acupuncture Society.* **27**, 150–154 (2009).
20. Ibarra, J. M. *et al.* Latent myofascial trigger points are associated with an increased antagonistic muscle activity during agonist muscle contraction. *J Pain.* **12**, 1282–1288 (2011).
21. Lucas, K. R., Rich, P. A. & Polus, B. I. Muscle activation patterns in the scapular positioning muscles during loaded scapular plane elevation: The effects of latent myofascial trigger points. *Clin Biomech.* **25**, 765–770 (2010).
22. Bohlooli, N., Ahmadi, A., Maroufi, N., Sarrafzadeh, J. & Jaberzadeh, S. Differential activation of scapular muscles, during arm elevation, with and without trigger points. *Journal of bodywork and movement therapies.* **20**, 26–34 (2016).
23. Bizzi, E. & Cheung, V. C. The neural origin of muscle synergies. *Frontiers in computational neuroscience.* **7**, 51 (2013).

24. Cheung, V. C. *et al.* Stability of muscle synergies for voluntary actions after cortical stroke in humans. *Proc Natl Acad Sci USA* **106**, 19563–19568 (2009).
25. d'Avella, A., Portone, A. & Lacquaniti, F. Superposition and modulation of muscle synergies for reaching in response to a change in target location. *J Neurophysiol.* **106**, 2796–2812 (2011).
26. Dominici, N. *et al.* Locomotor primitives in newborn babies and their development. *Science.* **334**, 997–999 (2011).
27. Oliveira, A. S., Gizzi, L., Farina, D. & Kersting, U. G. Motor modules of human locomotion: Influence of emg averaging, concatenation, and number of step cycles. *Frontiers in human neuroscience.* **8**, 335 (2014).
28. Gizzi, L., Nielsen, J. F., Felici, F., Ivanenko, Y. P. & Farina, D. Impulses of activation but not motor modules are preserved in the locomotion of subacute stroke patients. *J Neurophysiol.* **106**, 202–210 (2011).
29. d'Avella, A. & Lacquaniti, F. Control of reaching movements by muscle synergy combinations. *Frontiers in computational neuroscience.* **7**, 42 (2013).
30. Muceli, S., Boye, A. T., d'Avella, A. & Farina, D. Identifying representative synergy matrices for describing muscular activation patterns during multidirectional reaching in the horizontal plane. *J Neurophysiol.* **103**, 1532–1542 (2010).
31. Clark, D. J., Ting, L. H., Zajac, F. E., Neptune, R. R. & Kautz, S. A. Merging of healthy motor modules predicts reduced locomotor performance and muscle coordination complexity post-stroke. *J Neurophysiol.* **103**, 844–857 (2010).
32. Cheung, V. C. *et al.* Muscle synergy patterns as physiological markers of motor cortical damage. *Proc Natl Acad Sci USA* **109**, 14652–14656 (2012).
33. Liew, B. X. W., Del Vecchio, A. & Falla, D. The influence of musculoskeletal pain disorders on muscle synergies—a systematic review. *PLoS ONE.* **13**, e0206885 (2018).
34. Lee, D. D. & Seung, H. S. Learning the parts of objects by non-negative matrix factorization. *Nature.* **401**, 788–791 (1999).
35. Farina, D., Arendt-Nielsen, L., Roatta, S. & Graven-Nielsen, T. The pain-induced decrease in low-threshold motor unit discharge rate is not associated with the amount of increase in spike-triggered average torque. *Clin Neurophysiol.* **119**, 43–51 (2008).
36. Buchmann, J. *et al.* Objective measurement of tissue tension in myofascial trigger point areas before and during the administration of anesthesia with complete blocking of neuromuscular transmission. *Clin J Pain.* **30**, 191–198 (2014).
37. Quintner, J. L. & Cohen, M. L. Referred pain of peripheral nerve origin: An alternative to the “myofascial pain” construct. *Clin J Pain.* **10**, 243–251 (1994).
38. Ge, H. Y. & Arendt-Nielsen, L. Latent myofascial trigger points. *Curr Pain Headache Rep.* **15**, 386–392 (2011).
39. Farina, D., Arendt-Nielsen, L., Merletti, R. & Graven-Nielsen, T. Effect of experimental muscle pain on motor unit firing rate and conduction velocity. *J Neurophysiol.* **91**, 1250–1259 (2004).
40. Hug, F., Hodges, P. W. & Tucker, K. J. Effect of pain location on spatial reorganisation of muscle activity. *J Electromyogr Kinesiol.* **23**, 1413–1420 (2013).
41. Falla, D., Gizzi, L., Tschapek, M. & Erlenwein, J. & F., P. Reduced task-induced variations in the distribution of activity across back muscle regions in individuals with low back pain. *Pain.* **155**, 944–953 (2014).
42. Gerwin, R. D. Diagnosis of myofascial pain syndrome. *Phys Med Rehabil Clin N Am.* **25**, 341–355 (2014).
43. Turpin, N. A., Guevel, A., Durand, S. & Hug, F. Effect of power output on muscle coordination during rowing. *Eur J Appl Physiol.* **111**, 3017–3029 (2011).
44. Rha, D. W. *et al.* Detecting local twitch responses of myofascial trigger points in the lower-back muscles using ultrasonography. *Arch Phys Med Rehabil.* **92**, 1576–1580 e1571 (2011).
45. Scalone, L. *et al.* Italian population-based values of eq-5d health states. *Value Health.* **16**, 814–822 (2013).
46. Huskisson, E. C. Measurement of pain. *Lancet.* **2**, 1127–1131 (1974).
47. Geri, T. *et al.* Rasch analysis of the neck bournemouth questionnaire to measure disability related to chronic neck pain. *J Rehabil Med.* **47**, 836–843 (2015).
48. Franchignoni, F. *et al.* Minimal clinically important difference of the disabilities of the arm, shoulder and hand outcome measure (dash) and its shortened version (quickdash). *J Orthop Sports Phys Ther.* **44**, 30–39 (2014).
49. Monticone, M. *et al.* Development of the italian version of the tampa scale of kinesiophobia (tsk-i): Cross-cultural adaptation, factor analysis, reliability, and validity. *Spine (Phila Pa 1976).* **35**, 1241–1246 (2010).
50. Meroni, R. *et al.* Rasch analysis of the italian version of pain catastrophizing scale (pcs-i). *J Back Musculoskeletal Rehabil.* (2014).
51. Myburgh, C., Larsen, A. H. & Hartvigsen, J. A systematic, critical review of manual palpation for identifying myofascial trigger points: Evidence and clinical significance. *Arch Phys Med Rehabil.* **89**, 1169–1176 (2008).
52. Gizzi, L., Muceli, S., Petzke, F. & Falla, D. Experimental muscle pain impairs the synergistic modular control of neck muscles. *PLoS ONE.* **10**, e0137844 (2015).
53. Barbero, M., Merletti, R. & Rainoldi, A. *Atlas of muscle innervation zones. Understanding surface electromyography and its applications.* (Springer Milan, 2012).
54. Beretta Piccoli, M. *et al.* Innervation zone locations in 43 superficial muscles: Toward a standardization of electrode positioning. *Muscle Nerve.* **49**, 413–421 (2014).
55. d'Avella, A., Portone, A., Fernandez, L. & Lacquaniti, F. Control of fast-reaching movements by muscle synergy combinations. *J Neurosci.* **26**, 7791–7810 (2006).
56. R Core Team. R: A language and environment for statistical computing. Vienna, Austria: R Foundation for Statistical Computing, (2015).
57. Sartori, M., Gizzi, L., Lloyd, D. G. & Farina, D. A musculoskeletal model of human locomotion driven by a low dimensional set of impulsive excitation primitives. *Frontiers in computational neuroscience.* **7**, 79 (2013).
58. Bates, D., Mächler, M., Bolker, B. & Walker, S. Fitting linear mixed-effects models using lme4. *Journal of Statistical Software.* **67**, 1–48 (2015).
59. Kuznetsova, A., Bruun Brockhoff, P. & Haubo Bojesen Christensen, R. LmerTest: Tests in liner mixed effects models. (2016).
60. Barton, K. Mumin: Multi-model inference. (2017).
61. Green, P. & MacLeod, C. Simr: An r package for power analysis of generalised linear mixed models by simulation. *Methods in Ecology and Evolution.* **7**, 493–498 (2016).
62. Fox, J. & Weisberg, S. *An r companion to applied regression.* 2nd edn (Sage, 2011).

Acknowledgements

The authors wish to thank Dr. Giacomo Rossetini for his precious comments on an advanced version of the manuscript.

Author contributions

Design of the study: T.G., L.G., A.D.M. and M.T. Data collection: T.G. and A.D.M. Data Analysis: T.G., L.G. and A.D.M. Statistical Analysis: T.G. Data Interpretation: T.G., L.G. and M.T. Figures and Tables preparation: T.G. and L.G. Manuscript writing: T.G. and L.G. Manuscript revision and acceptance: T.G., L.G., A.D.M. and M.T.

Competing interests

The authors declare no competing interests.

Additional information

Supplementary information is available for this paper at <https://doi.org/10.1038/s41598-019-52561-3>.

Correspondence and requests for materials should be addressed to T.G.

Reprints and permissions information is available at www.nature.com/reprints.

Publisher's note Springer Nature remains neutral with regard to jurisdictional claims in published maps and institutional affiliations.



Open Access This article is licensed under a Creative Commons Attribution 4.0 International License, which permits use, sharing, adaptation, distribution and reproduction in any medium or format, as long as you give appropriate credit to the original author(s) and the source, provide a link to the Creative Commons license, and indicate if changes were made. The images or other third party material in this article are included in the article's Creative Commons license, unless indicated otherwise in a credit line to the material. If material is not included in the article's Creative Commons license and your intended use is not permitted by statutory regulation or exceeds the permitted use, you will need to obtain permission directly from the copyright holder. To view a copy of this license, visit <http://creativecommons.org/licenses/by/4.0/>.

© The Author(s) 2019